USE OF SPECTRAL DISTANCE, SPECTRAL ANGLE, AND PLANT ABUNDANCE DERIVED FROM HYPERSPECTRAL IMAGERY TO CHARACTERIZE CROP GROWTH VARIATION

C. Yang

Kika de la Garza Subtropical Agricultural Research Center
USDA-ARS
Weslaco, Texas

ABSTRACT

Vegetation indices (VIs) derived from remote sensing imagery are commonly used to quantify crop growth and yield variations. As hyperspectral imagery is becoming more available, the number of possible VIs that can be calculated is overwhelmingly large. The objectives of this study were to examine spectral distance, spectral angle and plant abundance derived from all the bands in hyperspectral imagery and compare them with eight widely used two-band or three-band VIs based on selected wavelengths for quantifying crop growth variability. Airborne hyperspectral images and yield monitor data collected from two grain sorghum fields were used for this study. A total of 64 VI images were generated based on the eight VIs and selected wavelengths for each field. Two spectral distance images, two spectral angle images and a pair of plant and soil abundance images were also created based on a pair of pure plant and soil reference spectra for each field. Correlation analysis showed that the modified soil-adjusted vegetation index (MSAVI) produced more consistent and higher r-values with yield than the other VIs among the selected bands. Spectral distance, spectral angle and abundance produced similar r-values to the VIs. The results from this study suggest that either a MSAVI image based one NIR band and one green band or a plant abundance image based on a pair of pure plant and soil spectra can be used to convert a hyperspectral image to a relative yield map.

Keywords: Hyperspectral imagery, Plant abundance, Spectral angle, Spectral distance, Vegetation index, Yield.

INTRODUCTION

Hyperspectral imagery contains tens to hundreds of bands of spectral data and therefore provides much finer spectral information than multispectral imagery. Traditionally, broad-band vegetation indices (VIs) derived from multispectral imagery are commonly used to characterize crop growing conditions and productivity such as leaf area index (LAI) (Baret and Guyot, 1991), chlorophyll content (Daughtry et al., 2000), biomass (Moran et al., 1995), and

yield (Wiegand et al., 1991; Yang and Anderson, 1999). These VIs are typically a sum, difference, ratio, or other combination of reflectance observations from two or more wavebands. The simple ratio index (SRI) (Jordan, 1969) and the normalized difference vegetation index (NDVI) (Rouse et al., 1973) derived from the red band and near-infrared (NIR) band are two of the earliest and most widely used VIs. More recently, many new VIs were developed to improve the linearity and sensitivity such as the modified simple ratio (MSR) (Chen et al., 1996) and the renormalized difference vegetation index (RDVI) (Rougean and Breon, 1995), and to compensate for the effect of soil background such as the soil-adjusted vegetation index (SAVI) (Huete, 1988) and the modified SAVI (MSAVI) (Qi et al., 1994). In addition to the two-band VIs, several three-band VIs were also developed, including the modified chlorophyll absorption in reflectance index (MCARI) (Daughtry et al., 2000), and the triangular vegetation index (TVI) (Broge and Leblanc, 2000). Haboudane et al. (2004) proposed two modified versions (MCARI1 and MCARI2) of MCARI and two modified TVI (MTVI1 and MTVI2) to lower the sensitivity to chlorophyll effects, increase the sensitivity to LAI changes, and reduce soil and atmospheric effects.

For a multispectral image which typically contains 3 bands as in SPOT 4 to 7 bands as in Landsat-7 ETM+, there are only one green band, one red band and one NIR band. The multispectral image can be easily converted to one single VI image based on the selected VI. However, a hyperspectral image contains dozens of red or NIR narrow bands and the number of VIs that can be calculated is overwhelmingly large. For example, if a hyperspectral image has 40 red bands and 50 NIR bands, the number of SRIs or NDVIs can be as many as 2000. Although computing technology has advanced, it is not always practical to calculate and examine all the possible VIs (i.e., the 2000 NDVI images in the example) to identify the best VI for a particular application. Therefore, the commonly-used multispectral VIs have been applied to hyperspectral imagery based on selected narrow bands. For example, the 800 nm and 670 nm narrow bands extracted from airborne hyperspectral imagery were used as the NIR band and red band, respectively, in the broadband VIs for estimating crop LAI (Haboudane et al., 2004) and crop yield (Zarco-Tejada et al., 2005). Other combinations of narrow bands derived from hyperspectral imagery have also been used for estimating crop growth parameters (Ray et al., 2006; Wu et al., 2010).

Thenkabail et al. (2000) used ground reflectance data measured in 490 discrete narrow bands between 350 and 1050 nm to characterize yield and other crop biophysical variables. They calculated narrow-band NDVI-type indices with all possible two-band combinations of the 490 bands and identified the best band centers and band widths for each crop variable. Based on the results from NDVIs and other hyperspectral indices, they recommended 12 hyperspectral bands for estimating agricultural crop biophysical information. Yang et al. (2004) applied stepwise regression analysis to grain yield monitor data and 102-band airborne hyperspectral imagery and identified four optimum bands for one field and seven different bands for a second field for estimating yield. Clearly, the identified optimum bands were the best for the particular datasets from which they were derived and may not be the best for different datasets. To avoid the need for band selection and make use of all the bands in hyperspectral imagery, Yang et al. (2007) used linear spectral unmixing to convert airborne hyperspectral imagery to

a single plant abundance image for quantifying the variation in crop yield. Yang et al. (2008) also applied spectral angle mapper (SAM) to airborne hyperspectral imagery to derive a single spectral angle image for the same purpose. Both linear spectral unmixing and SAM have been used commonly in remote sensing for image classification (Bateson and Curtiss, 1996; Dennison et al., 2004; Franke et al., 2009). Fractional abundance images determined by linear spectral unmixing may be preferred to NDVI as all the bands in the image are used (Bateson and Curtiss, 1996). Yang et al. (2007; 2008) demonstrated that both plant abundance images and spectral angle images provided better r-values with yield than most of the 5151 possible narrowband NDVIs derived from the 102-band hyperspectral images.

Crop yield is perhaps the most important piece of information for crop management in precision agriculture. Despite the commercial availability and increased use of yield monitors, most of the harvesters are not equipped with them. Relative yield maps derived from remote sensing imagery can be used as an alternative for both within-season and post-season management. Relative yield maps can be derived using any of the two-band and three-band VIs or the all-band plant abundance and spectral angle. Two or three center wavelengths have to be selected to calculate the VIs, while plant and soil endmembers need to be defined to derive plant abundance and spectral angle. Although many VIs are available and different center wavelengths have been suggested, it is still not clear which VIs and wavelengths should be used to convert a hyperspectral image to a relative yield map. Therefore, the first objective of this study was to compare five two-band VIs (SRI, NDVI, RDVI, SAVI and MSAVI) based on the 800 nm and 670 nm center wavelengths suggested by Haboudane et al. (2004) and three three-band VIs (MCARI1, TVI, and TVI2) for yield estimation. The second objective was to apply one NIR wavelength (825 nm) and eight visible wavelengths (495, 525, 550, 568, 668, 682, 696, and 720 nm) suggested by Thenkabail et al. (2000) to the five two-band VIs for yield estimation. The last objective was to relate yield to spectral distance, spectral angle and plant abundance and compare the correlations with those from the VIs.

METHODS

Hyperspectral Imagery and Yield Data

The airborne imagery and yield data collected from two grain sorghum fields (19 ha and 14 ha in size) in south Texas were used for this study. The description of the study sites, image acquisition, rectification, and calibration as well as yield data collection and processing is given in the article by Yang et al. (2008). The airborne imagery contained 102 usable bands with center wavelengths from 477.2 to 843.7 nm at 3.63 nm intervals. The swath of the imagery was 640 pixels and the radiometric resolution was 12 bits. The imagery was calibrated to reflectance (0-1) and resampled to 1 m spatial resolution. The yield data were aggregated to 9 m resolution (close to the effective cutting width of the harvester) and the number of aggregated yield samples was 2265 for field 1 and 1658 for field 2.

Hyperspectral Vegetation Indices

Eight VIs listed in Table 1 were selected as the hyperspectral VIs to be calculated for this study based on their performance for the estimation of LAI and yield by other researchers. The five two-band hyperspectral VIs (SRI, NDVI, RDVI, SAVI and MSAVI) were first calculated based on the 800 nm and 670 nm center wavelengths suggested by Haboudane et al. (2004) and the three three-band hyperspectral VIs (MCARI1, TVI, and TVI2) were calculated based on the center wavelengths given in the formulas.

Table 1. Vegetation indices calculated from hyperspectral imagery in this study.

Vegetation index	Equation	Reference
Simple ratio index (SRI)	$SRI=R_{NIR}/R_{Red}$	Jordan, 1969
Normalized difference vegetation index (NDVI)	$NDVI=(R_{NIR}-R_{Red})/(R_{NIR}+R_{Red})$	Rouse et al., 1973
Renormalized difference vegetation index (RDVI)	$RDVI=(R_{NIR}-R_{Red})/\sqrt{R_{NIR}+R_{Red}}$	Rougean and Breon, 1995
Soil-adjusted vegetation index (SAVI)	$SAVI=1.5(R_{NIR}-R_{Red})/(R_{NIR}+R_{Red}+0.5)$	Huete, 1988
Modified SAVI (MSAVI)	$MSAVI=0.5[2R_{NIR}+1-\sqrt{(2R_{NIR}+1)^2-8(R_{NIR}-R_{Red})}]$	Qi et al., 1994
Modified chlorophyll absorption in reflectance index (MCARI1)	$MCARI1=1.2[2.5(R_{800}-R_{670})-1.3(R_{800}-R_{550})]$	Haboudane et al., 2004
Triangular vegetation index (TVI)	$TVI=0.5[120(R_{750}-R_{550})-200(R_{670}-R_{550})]$	Broge and Leblanc, 2000
Modified TVI (MTVI2)	$MTVI2=\frac{1.5[1.2(R_{800}-R_{550})-2.5(R_{670}-R_{550})]}{\sqrt{(2R_{800}+1)^2-(6R_{800}-5\sqrt{R_{670}})-0.5)}}$	Haboudane et al., 2004

The second group of hyperspectral VIs was calculated based on the five two-band VIs using the center wavelengths suggested by Thenkabail et al. (2000). The 12 suggested center wavelengths include one blue band (495 nm), three green bands (525, 550, and 568 nm), three red bands (668, 682, and 696 nm), one red-edge band (720 nm), and four NIR bands (845, 920, 982, and 1025 nm). Because of the narrow spectral range of the hyperspectral data used in this study, there was no NIR center wavelength to match the four suggested NIR center wavelengths. Thenkabail et al. (2000) stated in the description of the suggested 845 nm wavelength that a broad band or a narrow band in the NIR shoulder (845±35) will provide the same results due to the near-uniform reflectance throughout the NIR shoulder. In order to examine the sensitivity of NIR wavelengths on the results,

the 810, 825 and 840 nm wavelengths were selected as the NIR band and the other eight visible bands as the red band in the NDVI formula to calculate the 24 possible NDVI-type indices as well as their correlations with yield for each field. The results showed that the three NIR wavelengths gave essentially the same results. Therefore, the 825 nm wavelength and the eight visible wavelengths were used to calculate hyperspectral indices based on the five two-band VIs.

Spectral Distance, Spectral Angle and Plant Abundance

Spectral distance is a spectral measure commonly used in unsupervised classification and supervised minimum distance classification (Campbell, 2002). The spectral distance between a pixel spectrum and a reference spectrum can be calculated by Euclidean distance as follows:

$$d = \sqrt{\sum_{i=1}^{n}(y_i - r_i)^2} \quad (1)$$

where d is the spectral distance, y_i is the reflectance in band i for a pixel, r_i is the reflectance in band i for a reference, and n is the number of bands in the image.

Spectral distance has the potential to quantify the variation in crop growth and yield. For example, if a pure healthy crop canopy is selected as the reference, the spectral distance between high-vigor plants and the reference will be small, whereas the spectral distance between low-vigor plants and the reference will be large. Therefore, spectral distance can be used as an indirect indicator of plant vigor.

Spectra angle is a spectral measure used in spectral angle mapper (SAM), a spectral classification technique that assigns pixels to classes based on the spectral angles between image pixel spectra and reference spectra (Kruse et al., 1993). The spectral angle between a pixel spectrum and a reference spectrum can be calculated by the following formula:

$$\alpha = \cos^{-1}\frac{\sum_{i=1}^{n} y_i r_i}{\sqrt{\sum_{i=1}^{n} y_i^2}\sqrt{\sum_{i=1}^{n} r_i^2}} \quad (2)$$

where α is the spectral angle between a pixel spectrum and a reference spectrum measured in radians or degrees, y_i is the reflectance in band i for the pixel, r_i is the reflectance in band i for a reference, and n is the number of bands in the image. Similar to spectral distance, spectral angle is also an indirect measure of plant vigor and abundance. When healthy crop canopy is selected as the reference, small angle values correspond to high-vigor plants and large values correspond to low-vigor plants.

Fractional plant cover or plant abundance within pixels can be estimated using linear spectral unmixing. Linear spectral unmixing models each spectrum in a pixel as a linear combination of a finite number of spectrally pure spectra of the components in the image, weighted by their fractional abundances (Adams et al., 1986; Garcia-Haro et al., 1996). If a component such as a healthy crop canopy or a bare soil surface occupies the whole pixel, then the pixel spectrum can be considered as the reference spectrum or endmember spectrum of the ground

component. For agricultural crop fields, crop plants and bare soil can be selected as the two meaningful ground components or endmembers for spectral unmixing analysis (Yang et al., 2007). Thus a simple linear spectral unmixing model has the following form:

$$y_i = r_{i1}x_1 + r_{i2}x_2 + \varepsilon_i, \quad i = 1, 2, \ldots, n \tag{3}$$

where y_i is the reflectance in band i for a pixel, r_{i1} and r_{i2} are the known reflectance in band i for pure crop plants and bare soil, respectively, x_1 and x_2 are the unknown fractional abundance for plants and soil, respectively, ε_i is the residual between actual and modeled reflectance for band i, and n is the number of spectral bands. This model is referred to as the unconstrained linear spectral unmixing model. For constrained linear spectral unmixing, x_1 and x_2 should sum to unity. In this study, only the unconstrained model was used.

To calculate plant abundance, a plant spectrum and a soil spectrum are needed. In comparison, only one reference spectrum is necessary to calculate spectral distance and spectral angle. Reference or endmember spectra can be obtained directly from the image or measured on the ground. In this study, healthy crop plants and bare soil were selected as the relevant endmembers. A pair of plant and soil spectra was extracted from each image to represent pure and healthy plants and bare soil for the respective field. To obtain pure spectra for crop plants, 50 pixels that had a bright red color on a color-infrared (CIR) image (corresponding to healthy plants and high yielding areas) were first identified from each image. Similarly, 50 pixels that contained pure bare soil were identified from each image (corresponding to non-vegetative and zero yielding areas). The endmember spectra for plants and soil for each image were obtained by averaging the spectra of the 50 respective training pixels from that image. Alternatively, computerized methods such as the pixel purity index and the n-dimensional visualizer in ENVI (Research Systems, Inc., Boulder, Colorado) can be used to identify purest pixels for the endmembers. However, these automatic methods are not always reliable. For example, weed plants can be mixed with crop plants and atypical soil surface areas with too dark or too bright colors can be misidentified as typical soil. Since there were only two endmembers in this particular application, the simple manual approach was used. Although only one reference spectrum is needed to calculate spectral distance and spectral angle, both the plant and soil spectra were used. Thus two spectral distance images, two spectral angle images, and two abundance images were calculated for each field based on the two reference spectra using ENVI.

Statistical Analysis

For correlation analysis, the 64 images based on the 10 VIs and the selected wavelengths and the six images based on the three hyperspectral measures (spectral distance, spectral angle and abundance) for each field were aggregated by a factor of 9 to match the 9-m yield data resolution. The digital value for each output cell was the mean of the 81 input cells that the 9 m × 9 m output cell encompassed. Correlation coefficients (r) between yield and each of the 70 spectral indices were calculated. Linear regression equations between yield and

selected spectral indices were also determined. SAS software (SAS Institute Inc., Cary, North Carolina) was used for statistical analysis.

RESULTS AND DISCUSSION

Table 2 gives the correlation coefficients between grain yield and the eight narrowband VIs for the two fields. The center wavelengths used to calculate SRI, NDVI, RNVI, SAVI, and MSAVI were 800 nm for the NIR band and 670 nm for the red band. The r-values ranged from 0.74 to 0.78 for field 1 and from 0.83 to 0.85 for field 2. Although all eight VIs provided similar results, RNVI, SAVI, MSAVI and MTV1 performed slightly better than SRI, NDVI, or MTV. The three three-band VIs (MCARI1, MTV, and MTV1) were not superior to the two-band VIs for yield estimation.

Table 2. Correlation coefficients (r) between grain yield and eight narrowband vegetation indices (VIs) derived from 102-band hyperspectral images for two grain sorghum fields.

Vegetation Index[a]	Field 1	Field 2
SRI	0.74[b]	0.83
NDVI	0.75	0.83
RNVI	0.77	0.85
SAVI	0.77	0.85
MSAVI	0.78	0.85
MCARI1	0.75	0.85
MTV	0.75	0.84
MTV1	0.76	0.85

[a] The eight VIs are defined in Table 1. The center wavelengths used to calculate SRI, NDVI, RNVI, SAVI, and MSAVI were 800 nm for the NIR band and 670 nm for the red band.

[b] All the r-values were significant at the 0.0001 level. The number of samples was 2265 for field 1 and 1658 for field 2.

Table 3 gives the correlation coefficients between grain yield and NDVI based on the three NIR bands (810, 825, 840 nm) and the eight visible bands for the two fields. For any visible center wavelength, the r-values were essentially the same among the three NIR center wavelengths, indicating that any of the NIR center wavelengths can be used. However, the r-values ranged from 0.74 to 0.80 for field 1 and from 0.82 to 0.85 for field 2 among the eight visible center wavelengths.

Table 4 summarizes the correlation coefficients between yield and the five two-band VIs based on the 825 nm center wavelength and the eight visible wavelengths for the two fields. Among the 40 VIs, the r-values varied from 0.73 to 0.80 for field 1 and 0.82 to 0.86 for field 2. Among the five VIs, RDVI, SAVI and MSAVI appeared to produce more consistent r-values than SRI or NDVI among the eight visible bands. For example, MSAVI provided similar r-values of 0.77-0.79 for field 1 and 0.85-0.86 for field 2 among the eight visible bands. The

commonly used NIR and red combinations were not the best for the two-band VIs for estimating crop yield. This result agrees with the findings of Thenkabail et al. (2000). The green bands tended to be better than the red bands, especially for SRI and NDVI. The red-edge band (720 nm) provided higher r-values than the red bands for field 1 and the highest r-values for field 2. However, the reflectance around this wavelength is very sensitive to the change in wavelength, so the r-values may not be stable. Therefore, MSAVI based on one NIR band (e.g., 825 nm) and one green band (e.g., 550 nm) appears to be one of the best VIs.

Table 3. Correlation coefficients (r) between grain yield and narrowband NDVI based on three NIR bands and eight visible bands derived from 102-band hyperspectral images for two grain sorghum fields.

Visible band center (nm)	NIR band center (Field 1)			NIR band center (Field 2)		
	810 nm	825 nm	840 nm	810 nm	825 nm	840 nm
495[a]	0.79[b]	0.79	0.79	0.82	0.82	0.82
525	0.80	0.80	0.80	0.82	0.82	0.82
550	0.80	0.80	0.80	0.83	0.83	0.83
568	0.79	0.78	0.79	0.83	0.83	0.83
668	0.75	0.75	0.75	0.83	0.83	0.83
682	0.74	0.74	0.74	0.83	0.83	0.83
696	0.75	0.75	0.75	0.83	0.83	0.83
720	0.79	0.78	0.78	0.85	0.85	0.85

[a] The NDVI-type indices were calculated with three NIR bands and eight visible bands. The red band in NDVI defined in Table 1 was replaced by the eight visible bands.

[b] All the r-values were significant at the 0.0001 level. The number of samples was 2265 for field 1 and 1658 for field 2.

Table 4. Correlation coefficients (r) between grain yield and five narrowband vegetation indices (VIs) derived from 102-band hyperspectral images for two grain sorghum fields.

Visible band center (nm)	Field 1					Field 2				
	SRI[a]	NDVI	RDVI	SAVI	MSAVI	SRI	NDVI	RDVI	SAVI	MSAVI
495	0.78[b]	0.79	0.78	0.77	0.78	0.82	0.82	0.84	0.84	0.85
525	0.80	0.80	0.79	0.78	0.78	0.83	0.82	0.85	0.85	0.85
550	0.80	0.80	0.79	0.79	0.79	0.85	0.83	0.85	0.85	0.85
568	0.78	0.78	0.79	0.79	0.79	0.85	0.83	0.85	0.85	0.85
668	0.74	0.75	0.77	0.77	0.77	0.83	0.83	0.85	0.85	0.85
682	0.73	0.74	0.76	0.76	0.77	0.83	0.83	0.85	0.85	0.85
696	0.73	0.75	0.77	0.77	0.77	0.84	0.83	0.85	0.85	0.85
720	0.78	0.78	0.79	0.79	0.79	0.86	0.85	0.86	0.86	0.86

[a] The narrowband indices were calculated with one NIR band (825 nm) and eight visible bands. The red band in the five VIs defined in Table 1 was replaced by the eight visible bands.

[b] All the r-values were significant at the 0.0001 level. The number of samples was 2265 for field 1 and 1658 for field 2.

Table 5 gives the correlation coefficients between grain yield and the three hyperspectral measures (spectral distance, spectral angle and abundance) derived from the 102-band hyperspectral images based on the plant and soil reference spectra for the two fields. Yield was negatively related to spectral distance and spectral angle and positively related to plant abundance based on the plant reference spectra. In contrast, yield was positively related to spectral distance and spectral angle, while negatively related to soil abundance based on the soil reference spectra. These r-values were within the ranges of the r-values for the 70 hyperspectral indices examined.

Table 5. Correlation coefficients (r) between grain yield and three hyperspectral measures (spectral distance, spectral angle and abundance) derived from 102-band hyperspectral images based on plant and soil reference spectra for two grain sorghum fields.

Hyperspectral measure	Field 1		Field 2	
	Plant-based	Soil-based	Plant-based	Soil-based
Spectral distance[a]	-0.76[b]	0.75	-0.85	0.84
Spectral angle	-0.77	0.77	-0.83	0.84
Abundance	0.78	-0.75	0.85	-0.82

[a] A pure plant spectrum and a pure soil spectrum extracted from each image were used to calculate spectral distance, spectral angle, and abundance.

[b] All the r-values were significant at the 0.0001 level. The number of samples was 2265 for field 1 and 1658 for field 2.

Yang et al. (2008) evaluated 10 different reference spectra for sorghum plants, soil, roads, and water extracted from hyperspectral images and from ground measurements for calculating spectral angle images. They found that spectral angle images based on reference spectra derived from bare soil, highway surface, or water provided similar or slightly better r-values than those derived from plants. Therefore, spectra for soil and other surfaces derived from the image can also be used to generate spectral angle images. When the soil spectra were used as the reference spectra for generating spectral angle images in this study, the r-values with yield were 0.77 for field 1 and 0.84 for field 2, compared with -0.77 and -0.83 for the respective fields based on the plant spectra (Table 5). Similarly, when the same soil spectra were used as the reference spectra for generating spectral distance images in this study, the r-values with yield were 0.75 for field 1 and 0.84 for field 2, which are similar to the r-values of -0.76 and -0.85 for the respective fields based on the plant spectra (Table 5).

Yang et al. (2007) examined how variations in endmember spectra affect plant abundance and its correlations with yield using 15 very different plant and soil spectrum pairs. Although the selection of the plant and soil endmember spectra affected the magnitude of the plant abundance values, the correlation coefficients between yield and unconstrained plant abundance were only

minimally affected. In their study, the r-values varied from 0.62 to 0.64 for one field and 0.79 to 0.81 for a second field among the 15 plant and soil spectrum pairs. In this study, the r-values between yield and unconstrained plant abundance were 0.78 for field 1 and 0.85 for field 2. Although the r-values for soil abundance (-0.75 for field 1 and -0.82 for field 2) are similar to those for plant abundance, it is more meaningful to use a plant abundance image as a relative yield map because plant abundance is a direct indicator of plant canopy cover.

Figures 1 and 2 show the scatter plots and regression lines of grain yield with (a) spectral distance, (b) spectral angle, (c) plant abundance, and (d) MSAVI derived from a 102-band airborne hyperspectral image for fields 1 and 2, respectively. Although there were clear linear correlations between yield and each of the four hyperspectral indices, there existed large variability in yield for any given value of each spectral variable. This is understandable because not every area with full canopy cover will have a high yield. Nevertheless, these general linear correlations with yield provide the basis for converting a hyperspectral image to a relative yield map using one of the spectral measures.

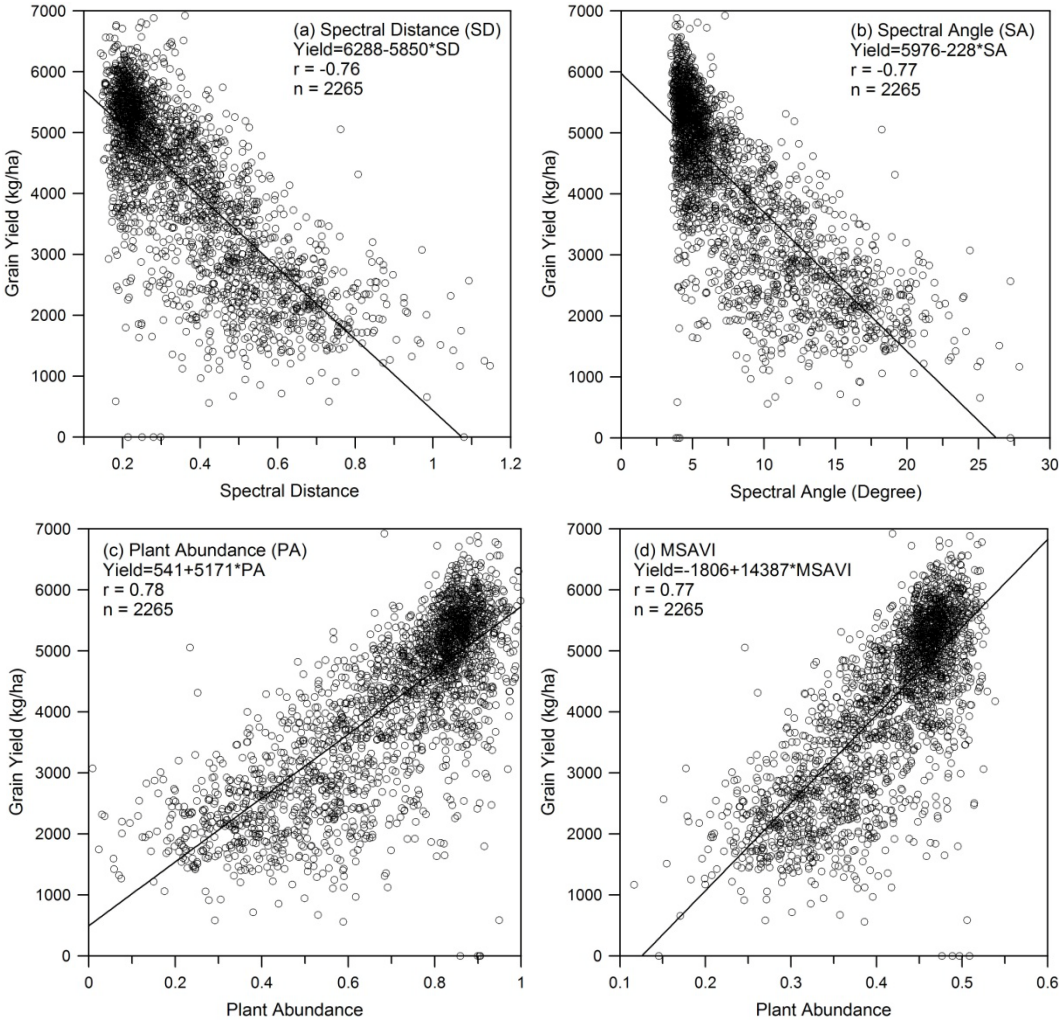

Fig. 1. Scatter plots and regression lines of grain yield with (a) spectral distance, (b) spectral angle, (c) plant abundance, and (d) MSAVI (NIR=825

nm and red =668) derived from a 102-band airborne hyperspectral image based on a reference plant spectrum for a grain sorghum field (field 1).

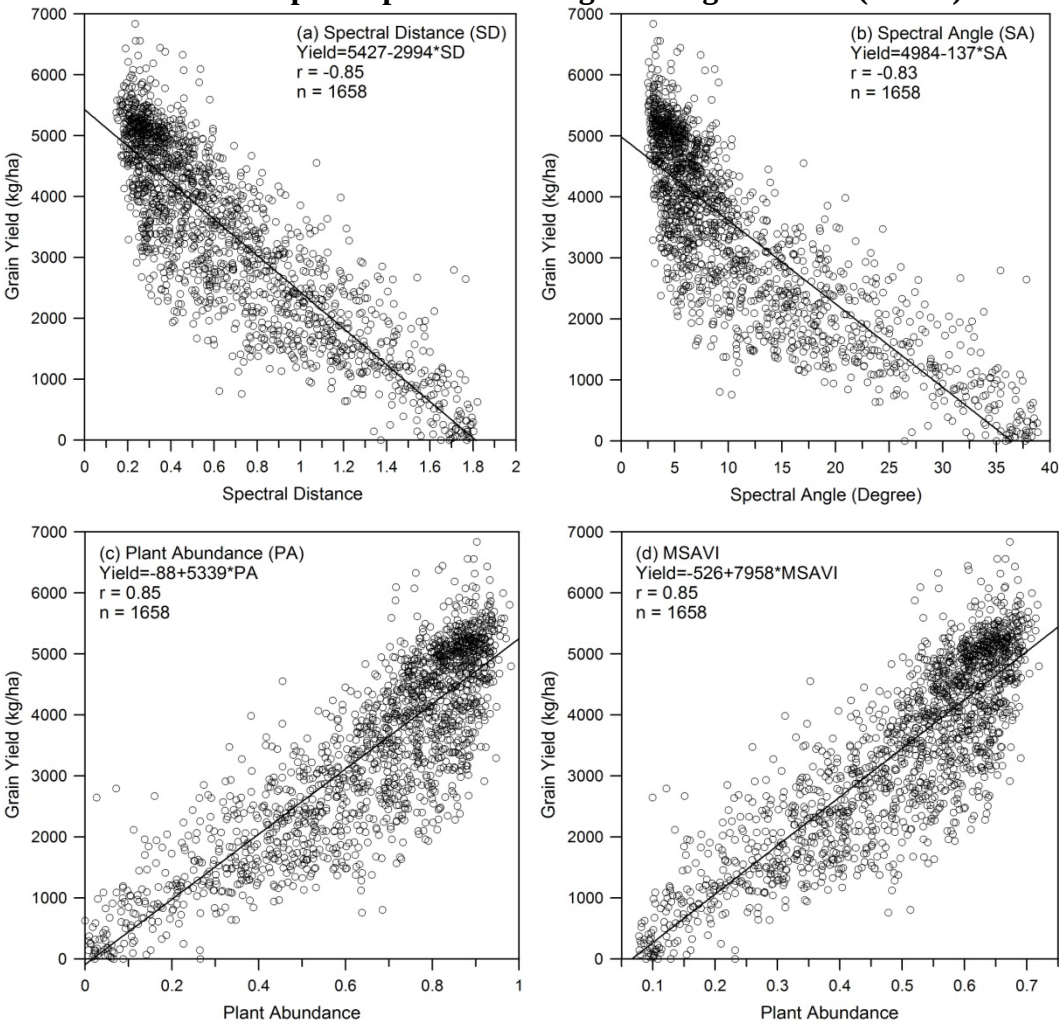

Fig. 2. Scatter plots and regression lines of grain yield with (a) spectral distance, (b) spectral angle, (c) plant abundance, and (d) MSAVI (NIR=825 nm and red =668) derived from a 102-band airborne hyperspectral image based on a reference plant spectrum for a grain sorghum field (field 2).

CONCLUSIONS

This study examined five two-band VIs (SRI, NDVI, RDVI, SAVI and MSAVI) and three three-band VIs (MCARI1, TVI, and TVI2) as well as three all-band hyperspectral measures (spectral distance, spectral angle and abundance) for yield estimation. MSAVI produced more consistent and generally higher r-values than the other VIs based on one NIR and eight visible wavelengths. The commonly used NIR and red combinations were not the best for the two-band VIs and the NIR and green band combinations tended to do better for yield estimation. The three all-band hyperspectral measures provided comparable results with the VIs. The three all-band hyperspectral measures do not need band selection, but

they require one or two reference spectra for the calculation. Compared with spectral distance and spectral angle, plant abundance provides a direct measure of crop canopy cover. This feature makes plant abundance even more attractive than traditional VIs. Therefore, to convert a hyperspectral image to a relative yield map, one can create a MSAVI image based one NIR band (e.g., 825 nm) and one green band (e.g., 550 nm) or a plant abundance image based on a pair of pure plant and soil spectra. More experiments are needed to validate these recommendations for other agricultural crops over diverse environments.

ACKNOWLEDGMENTS

The author thanks Rene Davis and Fred Gomez of USDA-ARS at Weslaco, TX for acquiring the imagery for this study and Jim Forward of USDA-ARS at Weslaco, TX for assistance in image rectification and calibration. Thanks are also extended to Bruce Campbell and Rio Farms, Inc. at Monte Alto, TX for use of their fields and harvest equipment.

REFERENCES

Adams, J. B., M. O. Smith, P. E. Johnson. 1986. Spectral mixture modeling: A new analysis of rock and soil types at the Viking Lander 1 site. Journal of Geophysical Research 91:8098-8112.

Baret, F., and G. Guyot. 1991. Potentials and limits of vegetation indices for LAI and APAR assessment. Remote Sens. Environ. 35:61-173.

Bateson, A. and B. Curtiss. 1996. A method for manual endmember and spectral unmixing selection. Remote Sensing of Environment 55:229-243.

Broge, N.H., and E. Leblanc. 2000. Comparing prediction power and stability of broadband and hyperspectral vegetation indices for estimation of green leaf area index and canopy chlorophyll density. Remote Sens. Environ. 76:156-172.

Campbell, J. B. 2002. Introduction to Remote Sensing, 3rd ed. The Guilford Press, New York.

Chen, J. 1996. Evaluation of vegetation indices and modified simple ratio for boreal applications. Can. J. Remote Sens. 22:229-242.

Daughtry, C.S.T., C.L. Walthall, M.S. Kim, E. Brown de Colstoun, and J.E. McMurtrey III. 2000. Estimating corn leaf chlorophyll concentration from leaf and canopy reflectance. Remote Sens. Environ. 74:229-239.

Dennison, P. E., K. Q. Halligan, and D. A. Roberts. 2004. A comparison of error metrics and constraints for multiple endmember spectral mixture analysis and spectral angle mapper. *Remote Sensing Environ.* 93(3): 359-367.

Franke, J., D. A. Roberts, K. Halligan, and G. Menz. 2009. Hierarchical Multiple Endmember Spectral Mixture Analysis (MESMA) of hyperspectral imagery for urban environments. Remote Sensing of Environment 113:1712-1723.

Garcia-Haro, F. J., M. A. Gilabert, and J. Melia. 1996. Linear spectral mixture modelling to estimate vegetation amount from optical spectral data. Int. J. Remote Sensing 17(17):3373-3400.

Haboudane, D., J.R. Miller, E. Pattey, P.J. Zarco-Tejada, and I. Strachan. 2004. Hyperspectral vegetation indices and novel algorithms for predicting green

LAI of crop canopies: Modeling and validation in the context of precision agriculture. Remote Sens. Environ. 90:337-352.

Jordan, C. F. 1969. Derivation of leaf area index from quality of light on the forest floor. Ecology 50(4):663-666.

Kruse, F. A., A. B. Lefkoff, J. W. Boardman, K. B. Heidebrecht, A. T. Shapiro, J. P. Barloon, and A. F. H. Goetz. 1993. The spectral image processing system (SIPS): Interactive visualization and analysis of imaging spectrometer data. Remote Sensing Environ. 44:145-163.

Moran, M. S., S. J. Maas, and P. J. Pinter Jr. 1995. Combining remote sensing and modeling for estimating surface evaporation and biomass production. Remote Sens. Environ. 12:335-353.

Qi, J., A. Chehbouni, A. R. Huete, Y. H. Keer, and S. Sorooshian. 1994. A modified soil vegetation adjusted index. Remote Sens. Environ., 48:119-126.

Ray, S. S., G. Das, J. P. Singh, S. Panigrahy. 2006. Evaluation of hyperspectral indices for LAI estimation and discrimination of potato crop under different irrigation treatments. International Journal of Remote Sensing 27(24):5373-5387.

Rougean, J.-L., and F.M. Breon. 1995. Estimating PAR absorbed by vegetation from bidirectional reflectance measurements. Remote Sens. Environ. 51:375-384.

Rouse, J. W., R. H. Haas, J. A. Shell, and D. W. Deering. 1973. Monitoring vegetation systems in the Great Plains with ERTS. In Proc. 3rd ERTS Symposium, 1: 309-317. NASA SP-351. Washington, D.C.: U.S. Government Printing Office.

Wiegand, C. L., A. J. Richardson, D. E. Escobar, and A. H. Gerbermann. 1991. Vegetation indices in crop assessments. Remote Sensing of Environment 35: 105-119.

Wu, C., X. Han, Z. Niu, J. Dong. 2010. An evaluation of EO-1 hyperspectral Hyperion data for chlorophyll content and leaf area index estimation. International Journal of Remote Sensing 31(4):1079-1086.

Yang, C. and G. L. Anderson. 1999. Airborne videography to identify spatial plant growth variability for grain sorghum. Precision Agriculture 1(1): 67-79.

Yang, C., J. H. Everitt, and J. M. Bradford. 2007. Airborne hyperspectral imagery and linear spectral unmixing for mapping variation in crop yield. Precision Agriculture 8(6):279-296.

Yang, C., J. H. Everitt, and J. M. Bradford. 2004. Airborne hyperspectral imagery and yield monitor data for estimating grain sorghum yield variability. Transactions of the ASAE 47(3):915-924.

Yang, C., J. H. Everitt, and J. M. Bradford. 2008. Yield estimation from hyperspectral imagery using spectral angle mapper (SAM). Transactions of the ASAE 51(2):729-737.

Zarco-Tejada P. J., S. L. Ustin, and M. L. Whiting. 2005. Temporal and spatial relationships between within-field yield variability in cotton and high-spatial hyperspectral remote sensing imagery. Agronomy Journal 97:641-653.